Research Article

Lucia Pirvu*, Georgeta Neagu, Iulian Terchescu, Bujor Albu, Amalia Stefaniu

Comparative studies of two vegetal extracts from *Stokesia laevis* and *Geranium pratense*: polyphenol profile, cytotoxic effect and antiproliferative activity

https://doi.org/10.1515/chem-2020-0098
received January 17, 2020; accepted March 24, 2020

Abstract: In this study, two ethanolic extracts, from *Stokesia aster* (Slae26) and *Geranium pratense* (Gpre36) respectively, were evaluated in order to assess the cytotoxic activity and potential antiproliferative activity upon the nontumorigenic human epithelial cell line derived from the mammary gland (MCF-12A) and the human breast tumor cell line (BT-20). The selection of the plant species was done on the basis of their chemical composition, specifically combinations of luteolin derivatives with caffeic and gallic acid derivatives. Therefore, the *S. laevis* ethanolic extract proved its capacity to inhibit the viability of both normal and tumor breast cell lines (i.e., up to 90% cell viability inhibition, IC_{50} = 42 μg/mL). On the contrary, the *G. pratense* ethanolic extract proved weak stimulatory effects on the viability of the two human breast cell lines studied. The obtained results were discussed in the contexts of computational studies and drug-likeness bioactivity of seven common luteolin derivatives: luteolin, luteolin-7-*O*-glucoside/cynaroside, luteolin-5-*O*-glucoside/galuteolin, luteolin-6-*C*-glucoside/isoorientin, luteolin-8-*C*-glucoside/orientin, luteolin-3′,4′-di-*O*-glucoside and luteolin-7,3′-di-*O*-glucoside. Computational studies have revealed that the hydrophilic behavior of luteolin derivatives (log *P* values) does not follow other tested parameters (e.g., polar surface area values), possibly explaining different efficacy concerning the biological properties *in vitro*. These predictions could be a starting point for studies on the biochemical mechanism by which luteolin derivatives induce biological effects.

Keywords: Stokes' aster, meadow cranesbill, cytotoxicity and antiproliferative effects, drug-likeness, bioactivity

1 Introduction

Scientific data of recent years indicate a greater attention to luteolin derivatives, especially as a result of *in vitro* evidence attesting their inhibitory potential upon breast (cancer) cell line development.

In this context, two ethanolic extracts found to contain luteolin derivatives aside caffeic and gallic/ellagic acid derivatives, from *Stokesia laevis* and *Geranium pratense* plant species, were studied concerning their *in vitro* cytotoxic activity and potential antiproliferative activity of two cell lines: a nontumorigenic epithelial cell line derived from mammary gland (MCF-12A) and a human breast tumor cell line (BT-20). The results were discussed in the context of computational studies and drug-likeness bioactivity of some of the most common luteolin derivatives usually found in plant species.

Regarding the two plant species selected, *S. laevis* (J. Hill; family *Asteraceae*), commonly known as "Stokes' aster", is a perennial species native to the United States (southeastern region) and mainly used as a decorative plant [1]. In the 1980s, there was an increased economical interest on this plant species as a result of Stokes' aster achenes content in vernolic acid, which is used in the chemical industry [2,3]; vernolic acid is an epoxide-type structured compound acting as a nonvolatile solvent useful for manufacturing oil-based paints, varnishes, adhesives and other industrial coatings. Data on the phytochemical composition and potential biological effects of *S. laevis* are scarce; the only data found argue the way in which the copigment luteolin and the pigments petunidin, pelargonidin and cyanidin result in the final coloration of *Stokesia aster* flower heads [1]. *Aster* species are reported to be nontoxic to dogs, except for the woody aster, *Xylorhiza orcuttii* [4].

* **Corresponding author: Lucia Pirvu,** National Institute of Chemical Pharmaceutical R&D (ICCF), Department of Pharmaceutical Biotechnology, 112 Vitan, Sector 3, Bucharest, Romania, e-mail: lucia.pirvu@yahoo.com
Georgeta Neagu, Iulian Terchescu: National Institute of Chemical Pharmaceutical R&D (ICCF), Department of Pharmacology, 112 Vitan, Sector 3, Bucharest, Romania;
Bujor Albu: National Institute of Chemical Pharmaceutical R&D (ICCF), Department of Physical Chemical Analysis and Quality Control, 112 Vitan Road, Sector 3, Bucharest, Romania;
Amalia Stefaniu: National Institute of Chemical Pharmaceutical R&D (ICCF), Department of Pharmaceutical Biotechnology, 112 Vitan Road, Sector 3, Bucharest, Romania

Geranium species (over 280 species are found worldwide) are particularly known for their geraniol (a volatile oil) and geraniin (a gallic/ellagic acid derivative) contents. The former has been shown to have antimicrobial [5–8] and antitumor potencies [9–11], while the latter shows augmented antioxidant and anti-inflammatory activities [12,13] and antitumor potency [14]. Geraniin compound also demonstrated antiviral properties on herpes simplex virus types 1 and 2 [15] and human enterovirus 71 [16] *in vitro* and the capacity to reduce the development of Alzheimer's disease by inhibiting β-secretase activity [17]. Geraniol has been proved to be an effective insecticidal and antimosquito compound [18]. Owing to their specific phytochemical content, the extracts from *Geranium* species proved to have numerous biological effects and health benefits on human. For example, *G. schiedeanum* extracts demonstrated hepatoprotective properties against ethanol-induced hepatic injuries [19]; *G. robertianum* and *G. molle* extracts showed toxicity against breast, lung, cervical and hepatocellular carcinomas [20,21]; *G. robertianum* demonstrated strong antioxidant and anti-inflammatory properties [22]; and *G. ayavacense* indicated antidiabetic activity [23]; while *G. carolinianum* demonstrated antiviral properties on hepatitis B virus [24].

G. pratense L. plant species (commonly known as "meadow cranesbill") are proved to be effective against free radical-induced impairment of endothelium-dependent relaxation in isolated rat aorta [25]. The methanol extract from the roots of *G. pratense* decreased the area with scab lesions on potato tubers; its impact against the pathogen *Streptomyces scabies* has been attributed to the antimicrobial activity of the geraniin compound [26]. The aqueous extract from the aerial part of *G. pratense* subsp. *finitimum* (Woronow) Knuth significantly inhibited the formation of carrageenan-induced hind paw edema (dose of 100 mg/kg) and also proved to have antinociceptive activity [27]. Finally, the *Encyclopedia of Traditional Chinese Medicine* recommends the utilization of the aerial parts of *G. pratense* in order to dispel wind damp, free channels and network vessels and treat dysentery and diarrhea [28].

2 Experimental procedure

2.1 Materials

2.1.1 Plant material description

S. laevis plant material was purchased from an authorized distributor in Romania, while *G. pratense* plant material was collected from Romanian Moldavian Carpathians. Taxonomic identification of the two plant species was done by the botanist's team at the National Institute of Chemical-Pharmaceutical R&D (ICCF), Bucharest, Romania. Voucher specimens (codified Sla26 and Gpr36) were deposited in the ICCF *Plant Material Storing Room*.

The two plant materials (the aerial part, *herba et flores*) were shade dried, ground to medium-size powder and then used in technological studies.

2.1.2 Vegetal extract preparation

S. laevis plant powder of 50 g was extracted with 1,000 mL of 70% (v/v) ethanol, after 1 h at the reflux temperature. After paper filtering, 750 mL of the whole ethanolic extract with a content of 0.70 mg gallic acid equivalent (GAE) per 1 mL extract was obtained. Furthermore, 300 mL of the whole ethanolic extract was concentrated at the residue, which was dissolved into 42 mL of 40% (v/v) ethanol, and then filtered on a glass fiber filter. The resultant extract, codified as Slae26, presents as a homogeneous brown liquid having a content of 5 mg GAE per 1 mL sample.

Similarly, 50 g of *G. pratense* plant powder was extracted with 500 mL of 70% (v/v) ethanol solvent after 1 h at reflux temperature. The whole ethanolic extract of 330 mL with a content of 3.50 mg GAE per 1 mL extract was obtained. The whole ethanolic extract of 100 mL was further concentrated as the residue, which was dissolved into 70 mL of 40% (v/v) ethanol and then filtered on the glass fiber filter. The resultant extract, codified as Gpre36, presents as a homogeneous light brown liquid with the exact content of 5 mg GAE per 1 mL sample.

The standardized extracts, Slae26 and Gpre36, were used in pharmacological studies.

Figure 1 shows the general method for obtaining the two standardized extracts.

2.1.3 Chemicals, reagents and references

Chemicals (aluminum chloride, sodium carbonate and sodium acetate), reagents (*Folin–Ciocalteu*, *Natural Product*-NP/PEG), solvents (ethanol, ethyl acetate, formic acid and glacial acetic acid) as well as the reference (ref.) compounds (rutin of min. 95%, quercitrin-3-*O*-rhamnoside >90%, luteolin >98%, luteolin-7-*O*-glucoside >98%, luteolin-8-*C*-glucoside >97%, caffeic acid 99%, chlorogenic acid >95% and gallic acid 95%) were purchased from Sigma-Aldrich, Romania. Cell culture reagents, Dulbecco's Modified Essential Medium, fetal bovine serum and antibiotics were also purchased from Sigma-Aldrich, Romania.

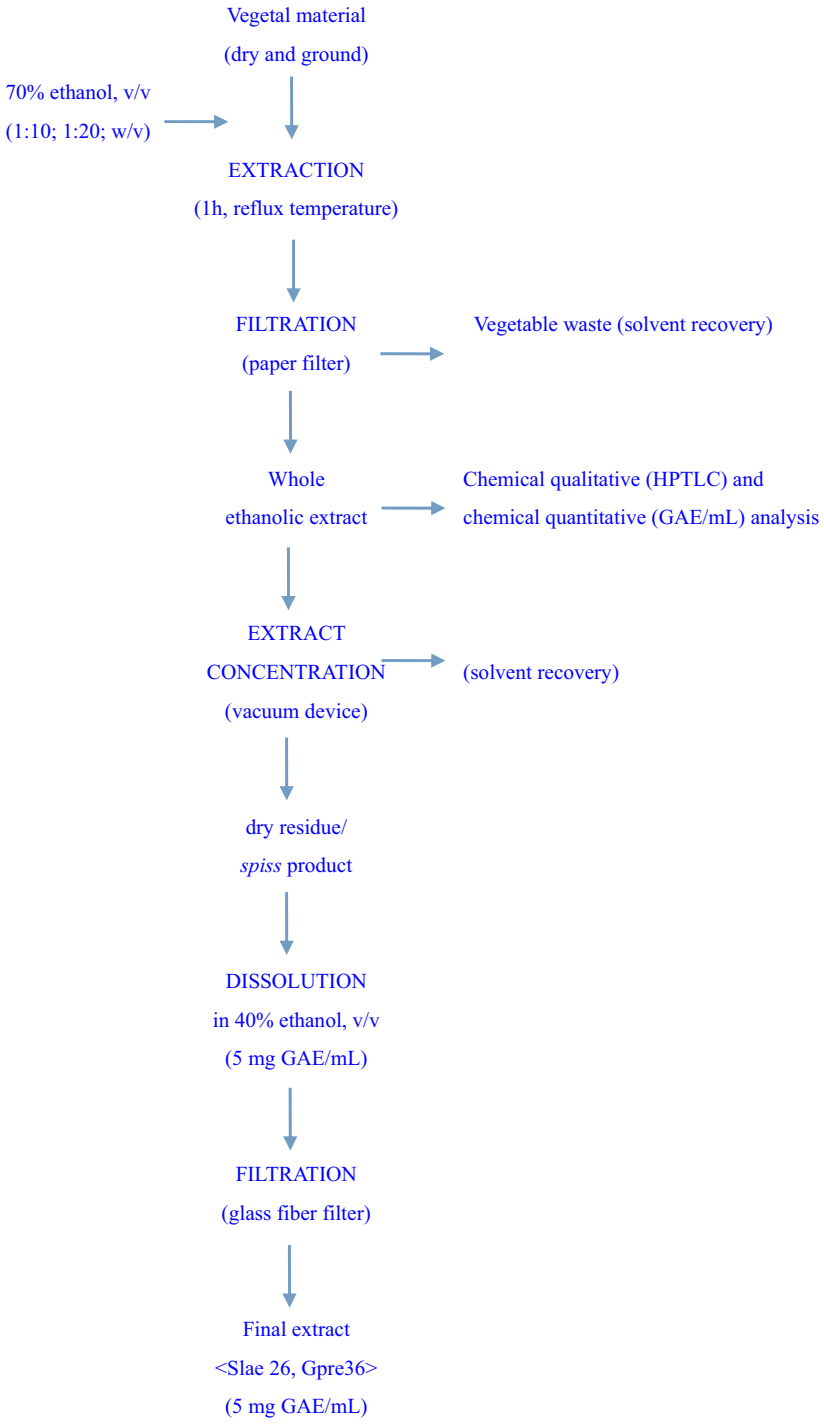

Figure 1: General method for the preparation of vegetal extracts.

2.2 Experimental design

2.2.1 Estimation of total phenol content in the test vegetal extracts

The total phenol content was estimated by the *Folin–Ciocalteu* reagent, the standard method described in *Romanian Pharmacopoeia* [29], and the results were expressed as milligram GAEs per 1 mL sample (R^2 = 0.970).

2.2.2 Qualitative high-performance thin-layer chromatography [(HP)TLC] analysis of test vegetal extracts

Chemical qualitative analyses were performed according to Wagner and Bladt [30] and Reich and Schibli [31]

chromatography atlases using two solvent systems: system A (ethyl acetate–glacial acetic acid–formic acid–water/100:12:12:26) recommended for polyphenol assessment and system B (chloroform–glacial acetic acid–methanol–water/64:32:12:8) used for saponin assessment, as described in the work of Pirvu et al. (first author of this study) [32].

2.2.3 *In vitro* pharmacological studies

The cell lines selected for *in vitro* pharmacological studies consisted of the nontumorigenic epithelial cell line derived from mammary gland MCF-12A (ATCC CRL-10782) and the human breast tumor cell line BT-20 (ATCC HTB-19).

The evaluation of *in vitro* cell cytotoxicity and antiproliferative effects was done by the MTS test (also known as the viability test), according to the Technical Bulletin of *Promega Corporation CellTiter 96 AQueous One Solution Cell Proliferation Assay* [33], as described in the work of Pirvu et al. (first author of this study) [34]. The MTS test allows evaluation of either the cytotoxic effect or the antiproliferative effect. For the (anti) proliferation assay, the application of the modulating factor (in this case the two vegetal extracts, Slae26 and Gpre36) is done on "sub-confluent" cell cultures (about 30%), and the determination of the cell population is performed after at least one division cycle (population doubling interval); for the cytotoxicity assay, the cells are exposed to "semi-confluent" cultures (about 70%) and the activity is measured for a shorter time period, rather than a doubling time (usually 6–12 h). Briefly, each test vegetal extract and dilution point series were prepared as triplicates and compared to a control sample with identical concentration of test vegetal solvent sample, at 40% (v/v) ethanol solution. After 20 h (cytotoxicity test) and 20 and 44 h (antiproliferative test) of exposure, the culture medium was removed. After another 2 h of incubation with the MTS solution, the viability of the adherent cells was determined *via* CellTiter 96 AQueous One Solution Cell Proliferation Assay (Promega, USA). The absorbance of the treated and control samples was measured at 490 nm with a Microplate Reader (Chameleon V Plate Reader; LKB Instruments, Australia) and the recorded values were used for cell viability estimation (see formula below). The results are calculated as mean ± SD, $n = 3$:

$$\%\ \text{cell viability} = \frac{A_{490}\ \text{of treated cells}}{A_{490}\ \text{of control cells}} \times 100.$$

2.2.4 Computational studies

Computational studies have been done on luteolin aglycone and several common luteolin derivatives/glucosides, namely, luteolin-7-*O*-glucoside/cynaroside, luteolin-5-*O*-glucoside/galuteolin, luteolin-6-*C*-glucoside/isoorientin, luteolin-8-*C*-glucoside/orientin, luteolin-3′,4′-di-*O*-glucoside and luteolin-7,3′-di-*O*-glucoside. Computational calculations have been carried out using Spartan '18 software [35,36], based on the density functional theory (DFT) using Becke's three-parameter hybrid functional with Lee, Yang, and Parr parameter (LYP) correlation functional (B3LYP) and 6.31G(d,p) basis sets [36,37]. The aims of DFT computations were to reveal site-selective and global chemical reactivity descriptors of the studied luteolin derivatives and to achieve a quantitative structure property relationship/quantitative structure-activity relationship (QSPR/QSAR) analysis of their calculated properties. The calculated properties were based on the optimized structures of molecules, thus presenting the configuration of minimum energy and an optimized geometry, in vacuum conditions; no solvent corrections were done. From their energy values, several descriptors important to assess the global chemical molecules reactivity were calculated by applying the Koopmans theorem [38,39], with the following relations: ionization potential ($I = -E_{HOMO}$), electron affinity ($A = -E_{LUMO}$), electronegativity ($\chi = (I + A)/2$), global hardness ($\eta = (I - A)/2$), local softness ($\sigma = 1/\eta$) [40,41], chemical potential ($\mu = (E_{HOMO} + E_{LUMO})/2$) and global electrophilicity index ($\omega = \mu^2/2\eta$). Also, a drug-likeness analysis was done based on the structural features correlated with Lipinski's rule of five [42]. The molecular descriptors included in this approach were calculated, for comparison, using the Molinspiration online platform (https://www.molinspiration.com/). In addition, the bioactivity scores toward G protein-coupled receptor (GPCR) ligand, ion channel modulators, kinase inhibitors, nuclear receptor ligands, protease inhibitors and other enzyme targets were predicted online through the Molinspiration virtual screening toolkit miscreen. The results of the seven luteolin derivatives were compared and discussed.

2.2.5 Instruments used

The instruments used for chemical analyses included the UV/Vis spectrophotometer (Hélios γ; Thermo Electron Corporation, UK) and Linomat5 TLC visualizer (CAMAG, Muttenz, Switzerland). Pharmacological *in vitro* cell proliferation tests were done by xCELLigence®DP Real-Time Cell Analysis (ACEA Biosciences, USA).

Ethical approval: The conducted research is not related to either human or animal use.

3 Results and discussion

3.1 Polyphenol profile of the two-test vegetal extracts

In Figure 2, chromatograms A and B present the polyphenol profiles of *S. aster* ethanolic extract, i.e., Slae26 test sample. System A setting study of Slae26 test sample (chromatogram A, tracks T2) face to eight reference compounds (tracks T1, T3, T4, T5, T6 and T7), which indicated the occurrence of two main polyphenol classes: luteolin derivatives (yellow fluorescent/fl. spots s2, s4 and s8) and caffeic acid derivatives (blue fl. spots s1, s3, s5 and s6), mainly chlorogenic acid and several chlorogenic acid isomers, respectively. Proved to be very useful for separation and assessment of polyphenol aglycones[32]. Subsequently system B setting studies of the Slae26 test sample, before hydrolysis in 4 N HCl medium (chromatogram B, tracks T2) and after hydrolysis in 4 N HCl medium (chromatogram B, tracks T2H), both confirmed the presence of luteolin-7-*O*-glucoside/cynaroside (A/s4/Rf ~ 0.68 and B/s1/Rf ~ 0.36), luteolin (A/s8/Rf ~ 0.94 and B/s2/Rf ~ 0.72) and caffeic acid (A/S7Rf ~ 0.92/and B/s3, Rf ~ 0.76).

In Figure 3, chromatograms A, B and C present the polyphenol profile of the *G. pratense* ethanolic extract i.e., Gpre36 test sample, compared to several reference compounds (tracks T1, T3, T4 and T5). System A setting study of the Gpre36 extract (chromatogram A, tracks T2) reveals an important number of polyphenol compounds, namely, luteolin (yellow fl., spots s5, s8), ellagic (light blue fl., spots s1, s2 and s4) and caffeic acid (blue fl., spots s7 and s10) derivatives and at least one kaempferol derivative (blue-green fl., spot s11).

System B setting study of the Gpre36 test sample, before and after hydrolysis in 4 N HCl medium (chromatogram B, tracks T2 and chromatogram C, tracks T2H) confirmed the presence of gallic acid aglycone (intense blue-indigo fl. spot s7, Rf ~ 0.55) and condensed derivatives, ellagic acids (intense blue-indigo fl. spot s1, s2 and s4); chromatogram C also revealed augmented quantities of luteolin (yellow fl. spot s8, Rf ~ 0.75) and kaempferol (green-blue fl. spot s9, Rf ~ 86) aglycones as well as low quantities of caffeic acid aglycone (blue fl. spot s8′ covered by luteolin s8). Other high-performance liquid chromatography studies [25] of extracts of *G. pratense* indicated the presence of quercitrin-3-*O*-α-arabinopyranoside, quercitrin-3-*O*-β-glucopyranoside, quercitrin-3-*O*-β-galactopyranoside, quercitrin-3-*O*-(2-*O*-galloyl)-β-glucopyranoside, quercitrin-3-*O*-(2-*O*-galloyl)-β-galactopyranoside, kaempferol-3-*O*-β-galactopyranoside, kaempferol-3-*O*-β-glucopyranoside and also myricetin-3-*O*-(2-*O*-galloyl)-β-glucopyranoside and (−)-6-chloro-epicatechin polyphenols.

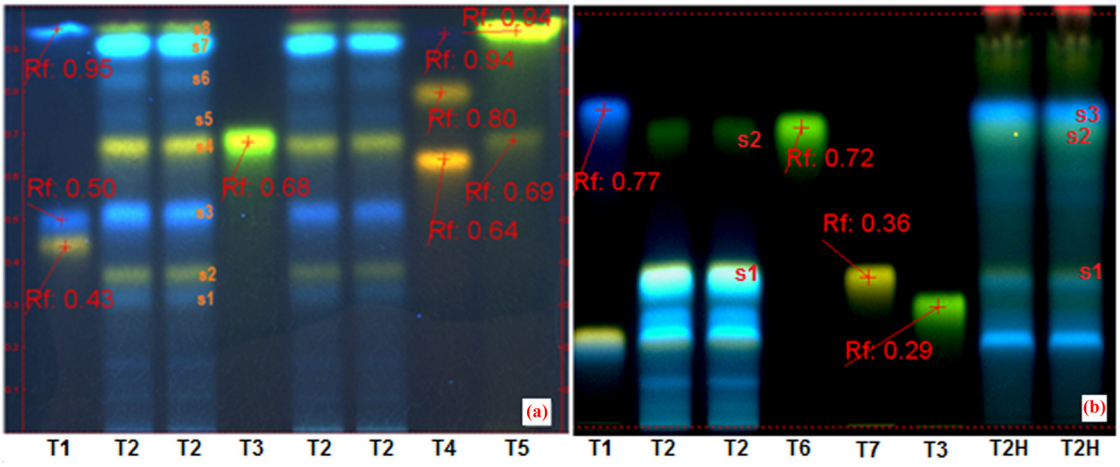

Figure 2: (HP)TLC studies of *Stokesia laevis* ethanolic extract (Slae26). Chromatogram A (system a) – track T1, rutin, chlorogenic acid and caffeic acid (ref.); tracks T2 – ethanolic extract from *S. laevis* (Slae26) – two series; track T3, luteolin-8-*C*-glucoside/orientin (ref.); track T4, quercitrin-3-*O*-galactoside/hyperoside, quercitrin-3-*O*-rhamnoside/quercitrin and gallic acid (ref.); track T5, luteolin-7-*O*-glucoside/cynaroside and luteolin (ref.). Chromatogram B (system b) – track T1, rutin, chlorogenic acid and caffeic acid (ref.); tracks T2 – ethanolic extract from *S. laevis* (Slae26); track T6, luteolin (ref); track T7, luteolin-7-*O*-glucoside/cynaroside (ref.); track T3, luteolin-8-*C*-glucoside/orientin (ref.); track T2H, the hydrolyzed extract from ethanolic extract Slae26.

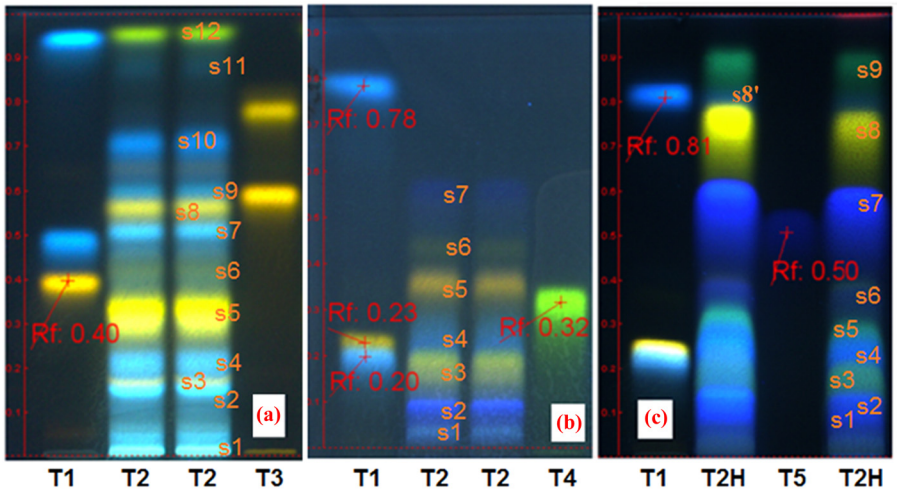

Figure 3: (HP)TLC studies of the *G. pratense* ethanolic extract (Gpre36). Chromatogram A (system a) – track T1, rutin, chlorogenic acid and caffeic acid (ref.); tracks T2, ethanolic extract from *G. pratens*e (Gpre36); track T3, quercitrin-3-*O*-glucoside/isoquercitrin and quercitrin-3-*O*-rhamnoside/quercitrin (ref.); chromatogram B (system b) – track T1, rutin, chlorogenic acid and caffeic acid (ref.); tracks T2 – ethanolic extract from *G. pratens*e (Gpre36); track T4, luteolin-8-*C*-glucoside/orientin (ref.); chromatogram C (system c) – track T1, rutin, chlorogenic acid and caffeic acid (ref.); track T2H, the hydrolyzed extract from ethanolic extract Gpre36; track T5, gallic acid (ref.).

By comparison, qualitative (HP)TLC studies revealed that the ethanolic extract from *S. aster* plant species, caffeic acid/s7, chlorogenic acid/s3 and one luteolin monoglycoside (likely luteolin-7-*O*-glucoside/s4) were found, and the ethanolic extract from *G. pratense* plant species confirmed numerous gallic/ellagic acid derivatives/s1, s2, s4 and one augmented luteolin polyglycoside/s5. Concerning the quantitative aspects, the two ethanolic extracts, Slae26 and Gpra36, were made in a manner to assure the exact content of 5 mg total phenol content, GAEs per 1 mL sample.

3.2 Cytotoxic and antiproliferative potential assays *in vitro*

In vitro cytotoxicity and antiproliferative assessments were done on Slae26 and Gpre36 test vegetal extracts (characterized by 5 mg GAE/mL sample) by using six dilution series, that is, 1, 5, 10, 25, 50 and 100 µg GAE/mL samples. The two test vegetal dilution series and the corresponding control sample dilution series (40% ethanol solvent series) were applied on "semi-confluent" and "sub-confluent" mammary gland cell culture MCF-12A and human breast tumor cell culture BT-20, as described in Section 2.2.3. As described, the cytotoxic and antiproliferative activities essentially consist in a colorimetric test based on the selective ability of the viable cells to reduce the tetrazolium component of MTS into a purple-colored formazan crystal; the quantity of the formazan product, as measured by absorbance at 490 nm, is directly proportional to the number of living cells in culture and thus the effect of the two-test vegetal series on the cytotoxic and proliferation tests can be computed as the cell viability percentage (%).

Figures 4 and 5 show the results on the *S. laevis* and *G. pratense* test vegetal extracts, Slae26 and Gpre36 dilution series, respectively.

Comparison with the control negative cell series indicated the following results: during cytotoxicity test, Slae26 test sample applied on the normal epithelial mammary gland cell line MCF-12A (Figure 3a) led to the stimulation of cell viability up to 50 µg/mL concentration level (up to 33% cell viability stimulation), followed by a severe decline in the cell viability at higher concentrations (up to 75% cell viability inhibition at 100 µg/mL); during the antiproliferative test, Slae 26 induced important inhibitory effects on MCF-12A viability (up to 52% and 70% cell viability inhibition at 24 and 48 h, respectively); Slae26 tested on human breast tumor cell line BT-20 (Figure 3b) revealed either cytotoxic effects (88% cell viability inhibition at 24 h) or antiproliferative activity (87% and 89% cell viability inhibition at 24 and 48 h, respectively), concluding that *Stokesia aster* ethanolic extract has inhibitory potential on the growth and proliferation of normal and tumor human breast cells. The antiproliferative effect (IC_{50}) was estimated at around values of 68 µg GAE/mL sample at 24 h and 42 µg GAE/mL sample at 48 h.

Due to the combination of luteolin derivatives with gallic or ellagic acid derivatives, which were shown to

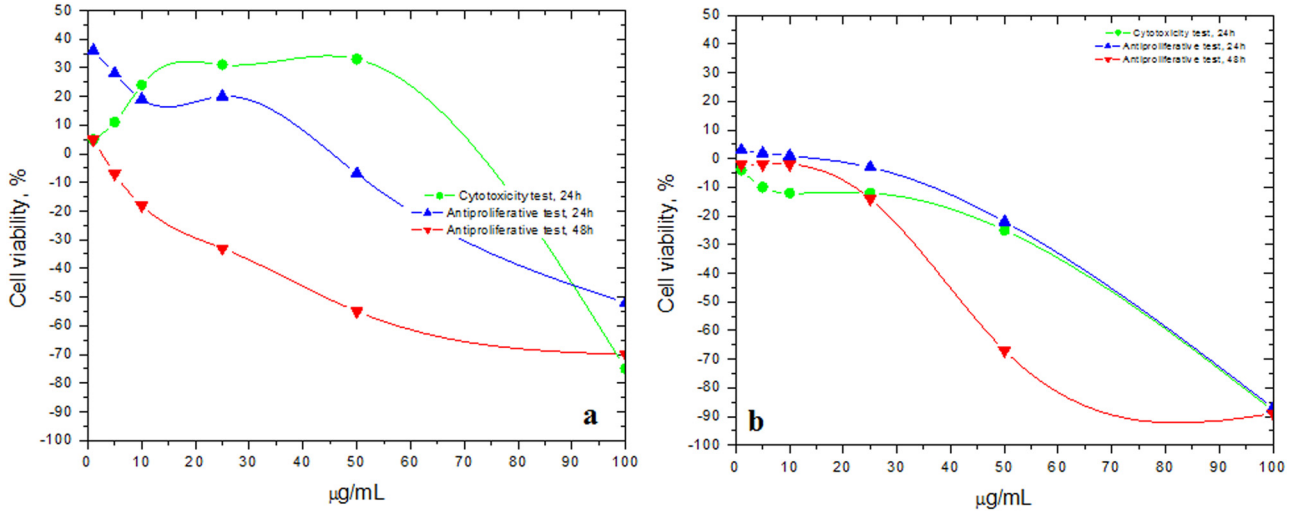

Figure 4: Cytotoxic and antiproliferative effects (cell viability, %) of Slae26 tested on (a) mammary gland cell line MCF-12A and (b) human breast tumor cell line BT-20, compared to the control negative cells; $n = 3$, ± SD(%).

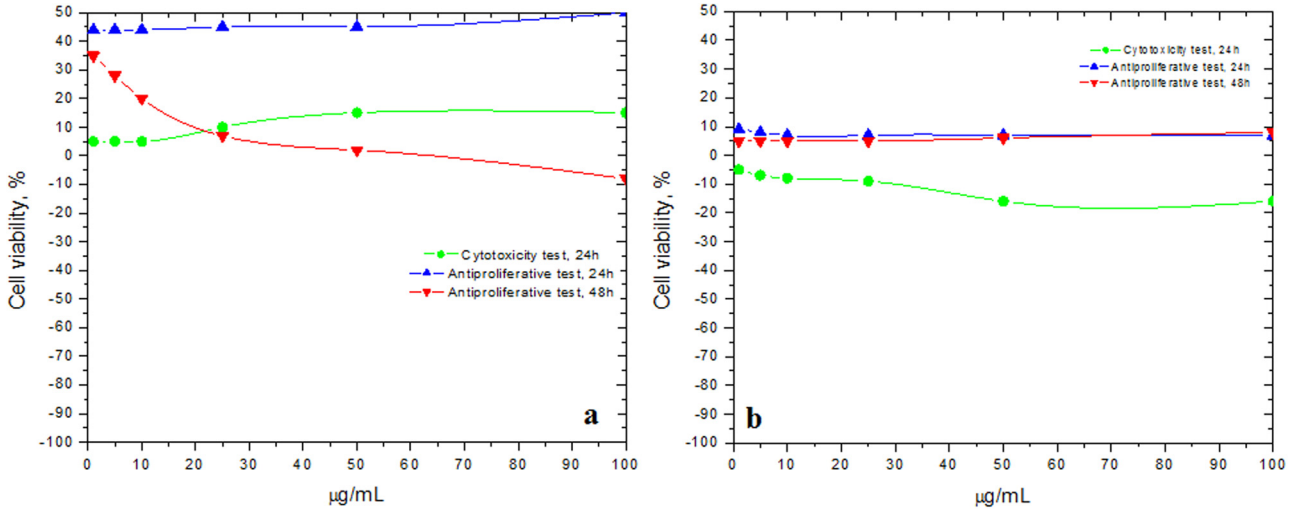

Figure 5: Cytotoxic and antiproliferative effects (cell viability, %) of Gpre36 tested on (a) mammary gland cell line MCF-12A and (b) human breast tumor cell line BT-20, compared to the control negative cells; $n = 3$, ± SD(%).

have strong antitumor, antimetastatic and antiangiogenesis activities [43,44], it is expected that the *G. pratense* ethanolic extract (Gpre36) has a strong antiproliferative potential. However, when applied on the normal mammary gland cell line MCF-12A (Figure 4a), it indicated a weak stimulatory activity in the cytotoxicity test (up to 15% cell viability stimulation); during the antiproliferative test, at first stimulatory effects were noticed (up to 50% cell viability stimulation at 24 h), followed by inhibitory effects (up to 8% cell viability inhibition at 48 h). Gpre36 test sample tested on human breast tumor cell line BT-20 (Figure 4b) indicated weak cytotoxic effects (up to 16% cell viability inhibition at 24 h), and no antiproliferative activity; in fact, 7% and 8% cell viability stimulatory effects were measured at 24 and 48 h, respectively. The results are available in Supplementary Tables 1s, 2s, 3s and 4s.

3.3 Computational results

Computational study of the seven luteolin derivatives, molecular descriptors and physicochemical properties was planned in order to find a possible explanation for the differences in pharmacological activity of the two-test vegetal extracts. Although the *G. pratense* ethanolic

extract has a theoretically more efficient chemical composition, *in vitro* assessments indicated the lack of antiproliferative activity of Gpre36 *versus* certain antiproliferative activity of *S. aster* ethanolic extract, Slae26. Therefore, it appears that the specific chemical structure of luteolin derivatives (the position and the number of substituents) and less combination with caffeic or gallic/ellagic acid derivatives lead to the final antiproliferative potential of the two vegetal extracts.

Table 1 summarizes the quantum chemical parameters for luteolin and the six most common luteolin derivatives: luteolin-7-*O*-glucoside/cynaroside, luteolin-5-*O*-glucoside/galuteolin, luteolin-6-*C*-glucoside/isoorientin, luteolin-8-*C*-glucoside/orientin, luteolin-3′,4′-di-*O*-glucoside and luteolin-7,3′-di-*O*-glucoside.

First of all, it is obvious that the energy of the highest occupied molecular orbital (HOMO) orbital (E_{HOMO}) of all studied compounds is significantly smaller than that of the energy of the lowest unoccupied molecular orbital (LUMO) orbital (E_{LUMO}). Energetically, from the HOMO orbital, it is easiest to donate electrons to form new bonds to be involved in oxidation. The LUMO is energetically more able to receive electrons, possibly involved in reduction reactions.

Second, the ΔE_{gap} parameter (the energy difference between HOMO and LUMO) providing information about chemical reactivity and kinetic stability of the molecules indicated close values, ranging between 4.14 and 4.26 eV.

Table 2 presents the values obtained for physicochemical properties and molecular descriptors involved when discussing the drug-likeness and matching with the statements of Lipinski's rule of five concerning oral bioavailability. For each structure, the first line of values corresponds to Spartan computations, and on the second line are the values obtained from the Molinspiration platform. A small difference is due to the methods used for computation. Molinspiration employed the semiempirical AM1 method for the optimized 3D molecular geometries, wherein volumes and polar surface area (PSA) are approximated based on the fragment contributions.

Table 2 clearly demonstrates luteolin aglycone as the most feasible drug candidate due to zero violation of Lipinski's rule [42]. Although not sufficient and mandatory to send a potential drug compound forward for pharmaceutical development, these limits of physicochemical parameters are used, rather than excluding from screening the compound with poor success rate. As observed from the results of computations, the correlation between the molecular weight and the PSA indicated that, generally, by increasing the molecular weight, from luteolin to luteolin diglucoside, the number of added hydroxyl groups and PSA increases. The biggest structures with the highest hydrophilicity, luteolin-3′,4′-diglucoside and luteolin-7,3′-di-glucoside, showed the most deviations from drug-likeness criteria (Lipinski's rule), also presenting the highest number of flexible bonds (*Nrotb*).

Yet, even if luteolin derivatives present a more augmented lipophilic character due to the lack of one hydroxyl group in position 3, the comparison of log *P* values (the calculated values of octanol–water partition coefficient log *P* by Spartan computations) with those

Table 1: Calculated quantum chemical parameters of the studied compounds

Studied parameter	Luteolin	Luteolin-7-*O*-glucoside/cynaroside	Luteolin-5-*O*-glucoside/galuteolin	Luteolin-6-*C*-glucoside/isoorientin	Luteolin-8-*C*-glucoside/orientin	Luteolin-3′,4′-di-*O*-glucoside	Luteolin-7,3′-di-*O*-glucoside
E_{HOMO}	−6.05	−6.00	−6.46	−6.09	−6.11	−6.20	−6.56
E_{LUMO}	−1.84	−1.82	−2.29	−1.83	−1.89	−1.89	−2.42
ΔE_{gap}	4.21	4.18	4.17	4.26	4.22	4.31	4.14
I	6.05	6.00	6.46	6.09	6.11	6.20	6.56
A	1.84	1.82	2.29	1.83	1.89	1.89	2.42
χ	3.94	3.91	4.37	3.96	4.00	4.04	4.49
η	2.105	2.09	2.08	2.13	2.11	2.15	2.07
σ	0.47	0.48	0.48	0.47	0.47	0.46	0.48
μ	−3.94	−3.91	−4.37	−3.96	−4.00	−4.04	−4.49
ω	3.68	3.66	4.59	3.68	3.79	3.79	4.87

E_{HOMO}, the energy of the HOMO orbital; E_{LUMO}, the energy of the LUMO orbital; ΔE_{gap}, difference between frontier molecular orbitals; I(ionization potential), $(-E_{HOMO})$; A (electron affinity), $(-E_{LUMO})$; χ (electronegativity), $(I + A)/2$; H (global hardness), $(I - A)/2$; σ (local softness), I/η; μ (chemical potential), $(E_{HOMO} + E_{LUMO})/2$ and ω (global electrophilicity index), $\mu^2/2\,\eta$, expressed in eV.

Table 2: Drug-likeness predicted parameters for luteolin and its derivatives[a]

Name	Molecular weight	Molecular volume	Nrotb	log *P*	PSA	HBD	HBA	No. of Lipinski violations
Luteolin[b] 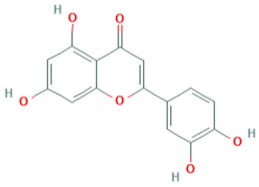	286.239	261.11 232.07	1	***−3.46*** *1.97*	97.416 111.12	4	6	**0**
Luteolin-7-O-glucoside[b]/cynaroside 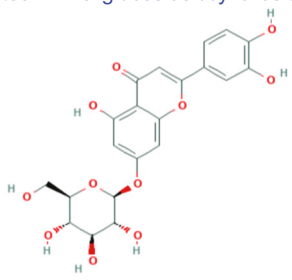	448.380	399.02 364.19	4	***−5.45*** *0.19*	168.657 190.28	7	11	**2**
Luteolin-5-O-glucoside[b]/galuteolin 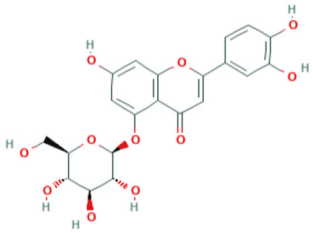	448.380	398.71 364.19	4	***−0.83*** *−0.07*	163.463 190.28	7	11	**2**
Luteolin-6-C-glucoside[b]/isoorientin 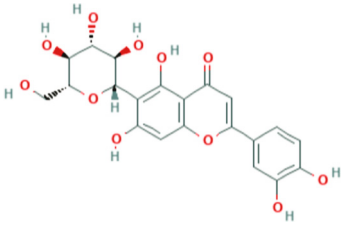	448.380	394.22 363.22	3	***−1.61*** *0.03*	164.602 201.27	8	11	**2**
Luteolin-8-C-glucoside[b]/orientin 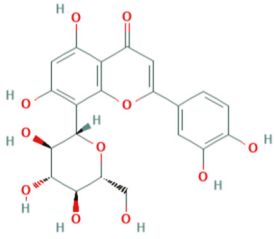	448.380	397.09 363.22	3	***−6.39*** *0.03*	178.988 201.27	8	11	**2**
Luteolin-3',4'-di-O-glucoside[c] 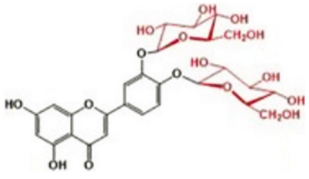	610.521	533.18	7	***−2.67***	214.904	10	16	**3**

Table 2: continued

Name	Molecular weight	Molecular volume	Nrotb	log *P*	PSA	HBD	HBA	No. of Lipinski violations
Luteolin-7,3'-di-O-glucoside[c] 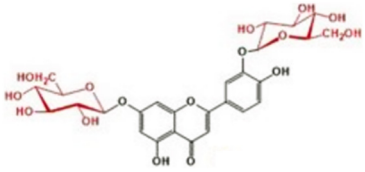	610.521	535.08 496.31	7	***–7.45*** *–1.83*	221.728 269.43	10	16	**3**

Nrotb, number of rotatable bonds; HBD, number of hydrogen bond donors; HBA, number of hydrogen bond acceptors; PSA, polar surface area; log *P*, water–octanol partition coefficient.
[a]Values on the first line were calculated using Spartan software and values listed on the second line were obtained using Molinspiration tools. [b]https://pubchem.ncbi.nlm.nih.gov/#query=luteolin. [c]https://tinyurl.com/qo2me42.

computed for quercitrin derivatives [34] indicates that (1) luteolin derivatives are more hydrophilic compounds capable of exhibiting greater oral bioavailability and (2) their log *P* values do not follow PSA values, possibly explaining their different efficacies concerning the biological properties and function of test conditions.

The correlation between PSA, molecular volume (vol) and water–octanol partition coefficient (log *P*) for the seven luteolin derivatives studied (Figure 6) indicated that luteolin, luteolin-5-*O*-glucoside, luteolin-6-*C*-glucoside and luteolin-3′,4′-*O*-diglucoside have significantly different log *P* values in comparison with luteolin-7-*O*-glucoside, luteolin-8-*C*-glucoside and luteolin-7,3′-*O*-diglucoside, which could support the differences between the pharmacological activity of the vegetal extracts.

In Table 3 are listed the bioactivity scores predicted using the Molinspiration software toward GPCR ligands, ion channel modulators, kinase inhibitors, nuclear receptor ligands, protease inhibitors and enzyme targets. It is known that if the bioactivity score is larger than 0.0, the drug candidate is classified as active; if score range is between –5 and 0, then the structure is moderately active and if the score is less than –5, then inactive. Therefore, luteolin exhibits larger score values for kinase inhibitor (0.26 – the largest of all the tested structures), nuclear receptor ligand (0.39, also the highest score, compared with its derivatives) and enzyme inhibitor

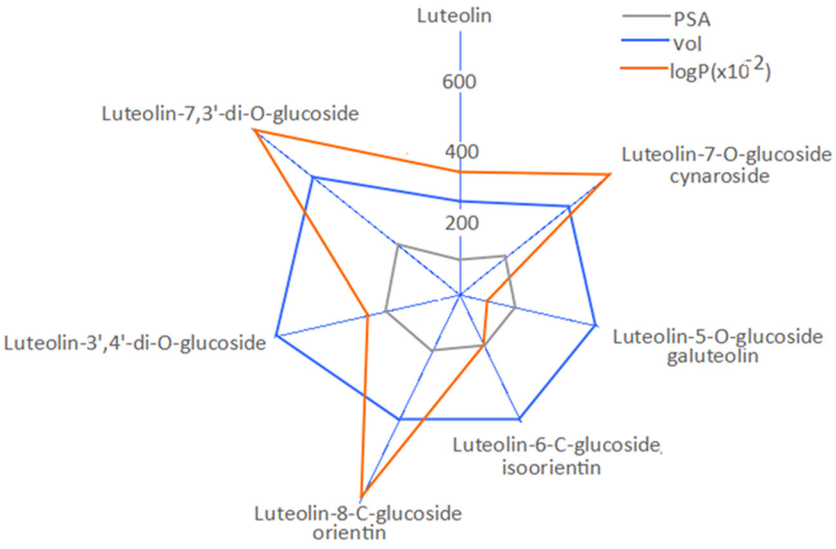

Figure 6: The correlation between molecular volume (vol), PSA and water–octanol partition coefficient (log *P*) for several common luteolin derivatives.

Table 3: Bioactivity scores for luteolin and its derivatives predicted with Molinspiration toolkit

Name/ChemSpider ID	GPCR ligand	Ion channel modulator	Kinase inhibitor	Nuclear receptor ligand bind	Protease inhibitor	Enzyme inhibitor
Luteolin ID 4444102	−0.02	−0.07	0.26	0.39	−0.22	0.28
Luteolin 7-*O*-glucoside/Cynaroside 4444241	0.09	−0.02	0.15	0.27	−0.01	0.42
Luteolin 5-*O*-glucoside/Galuteolin 10306091	0.12	0.00	0.18	0.29	−0.01	0.41
Luteolin 8-*C*-glucoside/Orientin 4444994	0.12	−0.14	0.20	0.20	0.01	0.45
Luteolin 6-*C*-glucoside/Isoorientin 102753	0.11	0.01	0.16	0.20	0.01	0.46
Luteolin-7,3′-di-*O*-glucoside 4590322	−0.03	−0.50	−0.11	−0.06	−0.04	0.07

(0.28), thus being considered as the most promising structure, the lead compound.

This conclusion is also supported by the results presented in Table 2, showing no deviation from the limiting criteria postulated by Lipinski's rule of five. On the contrary, luteolin-7,3′-di-*O*-glucoside, the most flexible molecule presenting seven rotatable bonds and three violations from Lipinski's rule (molecular weight larger than 500 Da; more than five hydrogen bond donors, more than ten hydrogen bond acceptors), shows the lowest scores for all targets. Thus, it is classified as a moderately active candidate. None of the luteolin derivatives can be considered inactive, as they all show scores larger than −5.0.

Table 3 also indicates that all compounds show greater scores for enzyme inhibition, all values being positives, acting as active drug candidates. Based on this, we can declare that the most active ligand is luteolin 6-*C*-glucoside with 0.46 score for enzyme inhibition. Concerning protease inhibition, the most active ones are luteolin 6-*C*-glucoside and luteolin 8-*C*-glucoside (score = 0.01). Luteolin aglycone is the most active when compared with its derivatives, because it is the ligand that is capable of binding to nuclear receptor (score = 0.39) and kinase inhibitor (score = 0.26). Luteolin 5-*O*-glucoside and luteolin 8-*C*-glucoside were found to be highly bioactive toward GPCR ligand (score = 0.12). Regarding ion channel modulator bioactivity, luteolin 6-*C*-glucoside shows a promising score (0.01).

Considering all the above observations of the drug-likeness parameters (Table 2) and bioactivities (Table 3), it can be concluded that all compounds show great potential in terms of bioactivity as ligands for the tested targets, starting with their lead compound, luteolin. Therefore, the interest in luteolin and luteolin derivatives in the recent years is argued. The advantages offered by luteolin derivatives as opposed to other flavonoid subclasses are drawn from their chemical structures: they are more resistant to the (auto)oxidation process explained by the lack of a hydroxyl group in position 3 of the flavan ring. They are resistant to acidic hydrolysis [32], at the same time more stable and safe and able to pass through the cell membranes more easily, while also showing great bioactivity potential.

Proving these, scientific data indicate that luteolin stimulates breast cancer cell apoptosis [45] and inhibits fatty acid synthase (FASN) activity [46–49], essential for normal and tumor breast cell growth and function. FASN is the only enzyme capable of inhibiting the *novo* synthesis of fatty acids with long chains (starting from acetyl-CoA, malonyl-CoA and nicotinamide adenine

dinucleotide phosphate). At the same time, it is significantly activated in many types of malignant tumors, especially in the case of human mammary tumor growth and metastasis.

Moreover, due to the complex actions that compete for the final effect, luteolin aglycone was proved to be an effective inhibitor of mammary and prostate cancer metastases [50]. For instance, luteolin inhibits the angiogenesis process induced by the vascular endothelial growth factor, which reduces the chance of colonization of metastatic targets [51]; luteolin inhibits the expression of specific matrix metalloproteinases involved in basement membrane degradation, a key step in the neovascularization and tumor invasion process [52]; luteolin inhibits the secretion of interleukin (IL)-8 [53] and IL-6, acting as an amplifying signal of cancer cell growth and invasion [54]; luteolin inhibits epithelial–mesenchymal transition considered as a pinnacle step in the process of cancer cell invasion and metastasis [55]; luteolin acts as a p90 ribosomal S6 kinase inhibitor that suppresses Notch4 signaling [56]; luteolin promotes cell cycle arrest in breast cancer and inhibits the expression of human epidermal growth factor receptors HER2 [57] and EGFR/aka HER1 [58], related to the new breast cancer cases; luteolin acts as an insulin-like growth factor-mediated proliferation antagonist [59] and stimulates breast cancer cell apoptosis through extrinsic (*via* caspase 9) [60] and intrinsic (via caspases 8 and 10) [61] pathways, thus being the subject of numerous review articles [62–64].

Regarding aspects of bioavailability, luteolin derivatives appear to be generally degraded to smaller metabolites by the intestinal bacterium *Eubacterium cellulosolvens* within 24 h; in contrast, luteolin C-polyglycosides appear unchanged when they are absorbed in the intestine, before being distributed to the body tissues [65].

Another aspect to be mentioned is the capacity of polyphenols, especially of flavonoid subclasses, to bind iron from the medium; flavonoid C-glycosides fulfil the role of siderophores in plant tissues [66,67]. The sequestration of iron from the intestine by polyphenol-based supplements leads to several shortcomings in humans: the inhibition of heme iron absorption possibly promotes anemia [68], the intestinal inflammation and colon tumor development. Data suggest that good intestinal bacteria are significantly affected by iron depletion. This is because their metabolism is dependent on numerous iron enzymes, while pathogenic bacteria necessitate low or no levels of iron to survive and proliferate [69]. A possible way to oppose iron sequestration by polyphenol-based supplements is by the addition of Fe and EDTA in tea in a molar ratio of 1:2, to avoid iron sequestration by green tea catechins [70].

4 Conclusion

The present study aims to evaluate the antiproliferative potencies of two vegetal extracts combining luteolin derivatives with caffeic and, respectively, gallic/ellagic acid derivatives isolated from *S. laevis* and *G. pratense* plant species.

In vitro pharmacological studies indicated that the ethanolic extracts of *S. laevis* have the ability to inhibit the viability of both sub-confluent and semi-confluent nontumorigenic epithelial mammary gland cell line MCF-12A and sub-confluent and semi-confluent human breast tumor cell line BT-20. This suggests both potential toxic effects and potential antiproliferative activity of human breast (cancer) cell development. Also, the fact that Stokes' aster ethanolic extract inhibited either normal or tumor breast cell line sustains the involvement of luteolin derivatives, which proved to inhibit the activity of FASN involved in both normal and tumor mammary cell metabolism.

G. pratense ethanolic extract yielded *in vitro* results that rather seem to suggest stimulatory effects on normal and tumor human breast cell development.

Computational studies made on luteolin and several common luteolin derivatives conducted to a reactivity analysis and to drug-likeness and bioactivity prediction approaches. For example, it was shown that luteolin, the structure that respects all limitations imposed by Lipinski's drug-likeness criteria, is a promising drug molecule, with a potential for higher activity against several biological targets. The predictions also indicate that all of its studied derivatives could exhibit good or moderate activity toward used receptors. The fact that log *P* values computed for luteolin derivatives do not follow the PSA values also explains to some extent the results of *in vitro* pharmacological studies, and antiproliferative effectiveness of Slae26 and Gpre36.

In summary, prediction studies are key factors for developing new drugs, giving a preview of the hydrophilic–lipophilic character, absorption, transport and distribution through the physiological media of the modeled compounds; it must be noticed that the computational scores are based on experimental data collected from the medicinal chemistry literature (about 10,000 data points for every target class) [71].

Overall, for the first time in the literature, the potential antiproliferative activity of the *S. aster* ethanolic extract was proved on tumor human breast cell line MT-20, but further studies are required to assess the exact chemical composition and to separate more active fractions to decrease the IC_{50} value. This way, the *S. laevis* plant species turns out to be a good source of luteolin derivatives for pharmaceutical purposes, but not for alimentary or phytomedicine purposes, since *in vitro* studies on the normal human epithelial mammary cell line MCT-12A indicate potential toxic effects (up to 88% cell viability inhibition) of the polar extracts from the aerial part of Stokes' aster.

Acknowledgments: This work was supported by the ANCSI program POC-A1-A1.2.3-G-2015, Project title <*New technologies and natural derived products for human health use*>, Contract no.60/05.09.2016, ID P_40_406, SMIS 105542.

Conflict of interest: The authors declare that this paper content has no conflict of interest.

References

[1] Barb JG, Werner DJ, Griesbach RJ. Genetics and biochemistry of flower color in Stokes aster. JASHS J Am Soc Horticult Sci. 2008;133:569–78.
[2] Campbell TA. Agronomic potential of Stokes aster. In: Pryde EH, Princen LH, Mukherjee KD, editors. New Sources of Fats and Oils. vol. 20, 1981. p. 287–96.
[3] Princen LH. New oilseed crops on the horizon. Econ Bot. 1983;37:478–92.
[4] https://www.ehow.com/info_12318214_asters-poisonous-dogs.html
[5] Pattnaik S, Subramanyam VR, Bapaji M, Kole CR. Antibacterial and antifungal activity of aromatic constituents of essential oils. Microbios. 1997;89:39–46.
[6] Edwards-Jones V, Buck R, Shawcross SG, Dawson MM, Dunn K. The effect of essential oils on methicillin-resistant *Staphylococcus aureus* using a dressing model. Burns. 2004;30:772–7.
[7] Lorenzi V, Muselli A, Bernardini AF, Berti L, Pages J-M, Amaral L, et al. Geraniol restores antibiotic activities against multidrug-resistant isolates from Gram-negative species. Antimicrob Agents Chemother. 2009;53:2209–11.
[8] Manu DK Graduate Theses and Dissertations, Iowa State University Capstones, Antimicrobial Activity of Cinnamaldehyde or Geraniol alone or Combined with High Pressure Processing to Destroy Escherichia coli O157:H7 and Salmonella enterica in Juice, 2016, https://lib.dr.iastate.edu/cgi/viewcontent.cgi?article=6976&context=etd
[9] Kim SH, Bae HC, Park EJ, Lee CR, Kim BJ, Lee S, et al. Geraniol inhibits prostate cancer growth by targeting cell cycle and apoptosis pathways. Biochem Biophys Res Commun. 2011;407:129–34.
[10] Chaudhary SC, Siddiqui MS, Athar M, Alam MS. Geraniol inhibits murine skin tumorigenesis by modulating COX-2 expression, Ras-ERK1/2 signaling pathway and apoptosis. J Appl Toxicol. 2013;33:828–37.
[11] Cho M, So I, Chun JH, Jeon JH. The antitumor effects of geraniol: modulation of cancer hallmark pathways (review). Int J Oncol. 2016;48:1772–82.
[12] Ito H, Iguchi A, Hatano T. Identification of urinary and intestinal bacterial metabolites of ellagitannin geraniin in rats. J Agric Food Chem. 2008;56:393–400.
[13] Ito H. Metabolites of the ellagitannin geraniin and their antioxidant activities. Planta Med. 2011;77:1110–5.
[14] OkaOkabe S, Suganuma M, Imayoshi Y, Taniguchi T, Fujiki H. New TNF-alpha releasing inhibitors, geraniin and corilagin, in leaves of Acer nikoense, Megusurino-ki. Biol Pharm Bull. 2001;24:1145–8.
[15] Yang CM, Cheng HY, Lin TC, Chiang LC, Lin CC. Ethnopharmacological communication. The *in vitro* activity of geraniin and 1,3,4,6-tetra-*O*-galloyl-β-D-glucose isolated from *Phyllanthus urinaria* against herpes simplex virus type 1 and type 2 infection. J Ethnopharmacol. 2007;10:555–8.
[16] Yang Y, Zhang L, Fan X, Qin C, Liu J. Antiviral effect of geraniin on human enterovirus 71 *in vitro* and *in vivo*. Bioorg Med Chem Lett. 2012;22:2209–11.
[17] Youn K, Jun M. *In vitro* BACE1 inhibitory activity of geraniin and corilagin from *Geranium thunbergii*. Planta Med. 2013;9:1038–42.
[18] Tabanca N, Wang M, Avonto C, Chittiboyina AG, Parcher JF, Carroll JF, et al. Bioactivity-guided investigation of geranium essential oils as natural tick repellents. J Agric Food Chem. 2013;61:4101–7.
[19] Madrigal-Santillán E, Bautista M, Gayosso-De-Lucio JA, Reyes-Rosales Y, Posadas-Mondragón A, Morales-González A, et al. Hepatoprotective effect of Geranium schiedeanum against ethanol toxicity during liver regeneration. World J Gastroenterol. 2015;21:7718–29.
[20] Graca VC, Barros L, Calhelha RC, Dias MI, Carvalho AM, Santos-Buelga C, et al. Chemical characterization and bioactive properties of aqueous and organic extracts of *Geranium robertianum* L. Food Funct. 2016;7:3807–14.
[21] Graca VC, Dias MI, Barros L, Calhelha RC, Santos PF, Ferreira IC. Fractionation of the more active extracts of *Geranium molle* L.: a relationship between their phenolic profile and biological activity. Food Funct. 2018;9:2032–42.
[22] Catarino MD, Silva AMS, Cruz MT, Cardoso SM. Antioxidant and anti-inflammatory activities of *Geranium robertianum* L. decoctions. Food Funct. 2017;8:3355–65.
[23] Aranda-Ventura J, Villacres J, Mego R, Delgado H. Effect of extracts of *Geranium ayavacense* W. (Pasuchaca) on glycemia on rats with experimental diabetes mellitus. Rev Peru Med Exp Salud Publica. 2014;31:261–6.
[24] Li J, Huang H, Zhou W, Feng M, Zhou P. Anti-hepatitis B virus activities of Geranium carolinianum L. extracts and identification of the active components. Biol Pharm Bull. 2008;31:743–7.

[25] Akdemir ZS, Tatli II, Saracoglu I, Ismailoglu UB, Sahin-Erdemli I, Calis I. Polyphenolic compounds from *Geranium pratense* and their free radical scavenging activities. Phytochemistry. 2001;56:189–93.
[26] Ushiki J, Tahara S, Hayakawa Y, Tadano T. Medicinal plants for suppressing soil-borne plant diseases. Soil Sci Plant Nutr. 1998;44:157–65.
[27] Kupeli E, Tatli II, Akdemir ZS, Yesilada E. Estimation of antinociceptive and anti-inflammatory activity on *Geranium pratense* subsp. finitimum and its phenolic compounds. J Ethnopharmacol. 2007;114:234–40.
[28] Zhou J, Xie G, Yan X. Encyclopedia of Traditional Chinese Medicines – molecular structures, pharmacological activities, natural sources and applications. Berlin Heidelberg: Springer-Verlag; 2011. vol. 5, 454 p.
[29] *Romanian Pharmacopoeia*, Xth ed., Medicala, Bucharest, 1993.
[30] Wagner H, Bladt S. Plant drug analysis. A thin layer chromatography atlas. 2nd ed. Berlin Heidelberg: Springer-Verlag; 1996.
[31] Reikh E, Schibli A. HPTLC for the analysis of Medicinal Plants. Thieme NY: Stuttgart; 2008.
[32] Pirvu L, Hlevca C, Nicu I, Bubueanu C. Comparative analytical, antioxidant and antimicrobial activity studies on a series of vegetal extracts prepared from eight plant species growing in Romania, JPC J Planar Chromatogr. 2014;27:346–56.
[33] https://www.promega.ro.pdf
[34] Pirvu L, Stefaniu A, Neagu G, Albu B, Pintilie L. *In vitro* cytotoxic and antiproliferative activity of *Cydonia oblonga* flower petals, leaves and fruits pellet ethanolic extracts. Docking simulation of the active flavonoids on anti-apoptotic protein Bcl-2. Open Chem. 2018;16:1–14.
[35] Shao Y, Molnar LF, Jung Y, Kussmann J, Ochsenfeld C, Brown ST, et al. Advances in methods and algorithms in a modern quantum chemistry program package. Phys Chem Chem Phys. 2006;8:3172–91.
[36] Hehre WJ. A guide to molecular mechanics and quantum chemical calculations. Irvine, CA: Wavefunction Inc.; 2003.
[37] Lee C, Yang W, Parr RG. Development of the Colle–Salvetti correlation–energy formula into a functional of the electron density. Phys Rev B. 1988;37:785–9.
[38] Sastri VS, Perumareddi JR. Molecular orbital theoretical studies of some organic corrosion inhibitors. Corros Sci. 1997;53:617–22.
[39] Yankova R, Genieva S, Halachev N, Dimitrova G. Molecular structure, vibrational spectra, MEP, HOMO–LUMO and NBO analysis of $Hf(SeO_3)(SeO_4)(H_2O)_4$. J Mol Struct. 2016;1106:82–88.
[40] Zarrouk A, Zarrok H, Salghi R, Hammouti B, Al-Dey ab SS, Touzani R, et al. A theoretical investigation on the corrosion inhibition of copper by quinoxaline derivatives in nitric acid solution. Int J Electrochem Sci. 2012;7:6353–64.
[41] Wang H, Wang X, Wang H, Wang L, Liu A. DFT study of new bipyrazole derivatives and their potential activity as corrosion inhibitors. J Mol Model. 2007;13:147–53.
[42] Lipinski CA, Lombardo F, Dominy BW, Feeney PJ. Experimental and computational approaches to estimate solubility and permeability in drug discovery and development settings. Adv Drug Delivery Rev. 2001;46:3–26.
[43] Moghtaderi H, Sepehri H, Delphi L, Attari F. Gallic acid and curcumin induce cytotoxicity and apoptosis in human breast cancer cell MDA-MB-231. Bioimpacts. 2018;8:185–94.
[44] Ceci C, Lacal PM, Tentori L, De Martino MG, Miano R, Graziani G. Experimental evidence of the antitumor, anti-metastatic and antiangiogenic activity of ellagic acid. Nutriets. 2018;10(11):E1756, doi: 10.3390/nu10111756
[45] Lin CH, Chang CY, Lee KR, Lin HJ, Chen TH, Wan L. Flavones inhibit breast cancer proliferation through the Akt/FOXO3a signaling pathway. BMC Cancer. 2015;15:958.
[46] Brusselmans K, Vrolix R, Swinnen JV. Induction of cancer cell apoptosis by flavonoids is associated with their ability to inhibit fatty acid synthase activity. J Biol Chem. 2005;280:5636–45.
[47] Günter S, Merfort I, Wölfle U, Schempp CM. Anti-carcinogenic effects of the flavonoid luteolin. Molecules. 2008;13:2628–51.
[48] Kuhajda FP. Fatty-acid synthase and human cancer: new perspectives on its role in tumor biology. Nutrition. 2000;16:202–8.
[49] Lupu R, Menendez JA. Pharmacological inhibitors of fatty acid synthase (FASN)-catalyzed endogenous fatty acid biogenesis: a new family of anti-cancer agents? Curr Pharm Biotechnol. 2006;7:483–49.
[50] Cook MT. Mechanism of metastasis suppression by luteolin in breast cancer. Breast Cancer Targets Ther. 2018;10:89–100.
[51] Cook MT, Liang Y, Besch-Williford C, Hyder SM. Luteolin inhibits lung metastasis, cell migration, and viability of triple-negative breast cancer cells. Breast Cancer. 2017;9:9–19.
[52] Sun DW, Zhang HD, Mao L, Mao CF, Chen W, Cui M, et al. Luteolin inhibits breast cancer development and progression *in vitro* and *in vivo* by suppressing notch signaling and regulating miRNAs. Cell Physiol Biochem. 2015;37:1693–711.
[53] Park SH, Kim JH, Lee DH, Kang JW, Song HH, Oh SR, et al. Luteolin 8-*C*-β-fucopyranoside inhibits invasion and suppresses TPA-induced MMP-9 and IL-8 via ERK/AP-1 and ERK/NF-κB signaling in MCF-7 breast cancer cells. Biochimie. 2013;95:2082–90.
[54] Tu DG, Lin WT, Yu CC, Lee SS, Peng CY, Lin T, et al. Chemotherapeutic effects of luteolin on radio-sensitivity enhancement and interleukin-6/signal transducer and activator of transcription 3 signaling repression of oral cancer stem cells. J Formos Med Assoc. 2016;115:1032–8.
[55] Lin D, Kuang G, Wan J, Zhang X, Li H, Gong X, et al. Luteolin suppresses the metastasis of triple-negative breast cancer by reversing epithelial-to-mesenchymal transition via downregulation of β-catenin expression. Oncol Rep. 2017;37:895–902.
[56] Reipas KM, Law JH, Couto N, Islam S, Li Y, Li H, et al. Luteolin is a novel p90 ribosomal S6 kinase (RSK) inhibitor that suppresses Notch4 signaling by blocking the activation of Y-box binding protein-1 (YB-1). Oncotarget. 2013;4:329–45.
[57] Lee EJ, Oh SY, Sung MK. Luteolin exerts anti-tumor activity through the suppression of epidermal growth factor receptor-mediated pathway in MDA-MB-231 ER-negative breast cancer cells. Food Chem Toxicol. 2012;50:4136–43.
[58] Chiang CT, Way TD, Lin JK. Sensitizing HER2-overexpressing cancer cells to luteolin-induced apoptosis through suppressing p21WAF1/CIP1 expression with rapamycin. Mol Cancer Ther. 2007;6:2127–38.

[59] Wang LM, Xie KP, Huo HN, Shang F, Zou W, Xie MJ. Luteolin inhibits proliferation induced by IGF-1 pathway dependent ERα in human breast cancer MCF-7 cells. Asian Pac J Cancer Prev. 2012;13:1431–7.
[60] Park SH, Ham S, Kwon TH, Kim MS, Lee DH, Kang JW, et al. Luteolin induces cell cycle arrest and apoptosis through extrinsic and intrinsic signaling pathways in MCF-7 breast cancer cells. J Env Pathol Toxicol Oncol. 2014;33:219–31.
[61] Yang MY, Wang CJ, Chen NF, Ho WH, Lu FJ, Tseng TH. Luteolin enhances paclitaxel-induced apoptosis in human breast cancer MDA-MB-231 cells by blocking STAT3. Chem Biol Interact. 2014;213:60–68.
[62] Kuhajda FP. Fatty acid synthase and cancer: new application of an old pathway. Cancer Res. 2006;66:5977–80.
[63] Pandey PR, Liu W, Xing F, Fukuda K, Watabe K. Anti-cancer drugs targeting fatty acid synthase (FAS). Recent Pat Anti-Cancer Drug Discovery. 2012;7:185–97.
[64] Zhang JS, Lei JP, Wei GQ, Chen H, Ma CY, Jiang HZ. Natural fatty acid synthase inhibitors as potent therapeutic agents for cancers: a review. Pharm Biol. 2016;54:1919–25.
[65] Xiao J, Capanoglu E, Jassbi AR, Miron A. Advance on the flavonoid C-glycosides and health benefits. Crit Rev food Sci Nutr. 2016;56:S29–45.
[66] Ma Q, Kim EY, Lindsay EA, Han O. Bioactive dietary polyphenols inhibit heme iron absorption in a dose-dependent manner in human intestinal Caco-2 cells. J Food Sci. 2011;76:H143–50.
[67] Hultin PG. Bioactive C-glycosides from bacterial secondary metabolism. Curr Top Med Chem. 2005;5:1299–331.
[68] Brazier-Hicks M, Evans KM, Gershater MC, Puschmann H, Steel PG, Edwards R. The C-glycosylation of flavonoids in cereals. J Biol Chem. 2009;284:17926–34.
[69] Ylmaz B, Li H. Gut microbiota and iron: the crucial actors in health and disease. Pharmaceuticals. 2018;11:98.
[70] Dueik V, Chen BK, Diosady LL. Iron–polyphenol interaction reduces iron bioavailability in fortified tea: competing complexation to ensure iron bioavailability. J Food Qual. 2017;2017:7.
[71] https://molinspiration.com/docu/miscreen/virtualscreening.html